Cells and Materials

Volume 2 | Number 4 Article 8

1992

# Projection Effect Errors in Biomaterials and Bone Research

K. N. Bachus
*Department of Veterans Affairs Medical Center, Salt Lake City*

R. D. Bloebaum
*Department of Veterans Affairs Medical Center, Salt Lake City*

CELLS AND MATERIALS, Vol. 2, No. 4, 1992 (Pages 347-355) 1051-6794/92$3.00+.00
Scanning Microscopy International, Chicago (AMF O'Hare), IL 60666 USA

# PROJECTION EFFECT ERRORS IN BIOMATERIALS AND BONE RESEARCH

K.N. Bachus* and R.D. Bloebaum

Bone and Joint Research Laboratories (151F)
Department of Veterans Affairs Medical Center,
500 Foothill Blvd., Salt Lake City, UT 84148 U.S.A.

(Received for publication December 5, 1992, and in revised form December 31, 1992)

## Abstract

Microradiography and backscattered electron (BSE) imaging are techniques used to investigate the morphologic, histometric, and mineral content changes at the bone/biomaterials interface. Investigators have shown that the superimposition of multiple tissue layers can cause errors with both the morphologic observations and the histometric measurements of bone. The objective of this study was to document errors in the bone mineral content measurements associated with overlapping tissues.

Using a digital image analysis system, microradiographic and BSE images from canine cortical and cancellous bone were captured and analyzed. The results of this study showed that microradiography had more projection effect errors associated with the morphology and histometry. The BSE technique provided substantially better resolution of the bone morphology and showed significantly more ($p \leq 0.05$) bone surface perimeter than the microradiographic technique. Contrary to the literature, the BSE images did not show less bone area than the microradiographic images of the identical regions. This discrepancy was explained by projection effect errors and over penetration artifacts of the X-ray beam.

Unique to this study was the documentation that microradiography has inherent projection effect errors associated with mineral content measurements. The BSE images had significantly more ($p \leq 0.05$) graylevels present than the microradiographic images. Due to the limited tissue overlap, the BSE images provide excellent morphologic resolution, accurate bone histometry and the ability to accurately measure the mineral content of cortical and cancellous bone at a microscopic level.

Key Words: Backscattered electron imaging; microradiography; projection effect errors; histometry; mineral content, bone, scanning electron microscope, cortical, cancellous, morphology.

*Address for correspondence:

Kent N. Bachus,
Bone and Joint Research Laboratories (151F)
VA Medical Center, Salt Lake City, UT 84148 U.S.A.
Telephone: (801)582-1565 x4696

## Introduction

Researchers are attempting to understand how biomaterials, mechanical loading, and pharmaceutics affect bone tissue at the microscopic level. However, progress towards understanding the microscopic changes that occur between bone and biomaterials have been limited by the inability to quantitatively correlate the morphology and histometry [42] with the mineral content [60, 67, 68].

Overlapping layers of tissue have been shown [11, 42, 72] to mask morphologic structures and to skew histometric measurements of bone -- especially cancellous bone. The magnitude of these projection effect errors is related to the thickness of the specimen being imaged. The thicker the specimen, the more overlapping layers are imaged and thus, the greater the potential for error. It was shown as early as the 1920s, when a geologist reported that when looking down onto multilayered objects, that the resulting boundary is defined by the widest projection of the overlapped structures [41].

There are many imaging methods that help investigators to study the microscopic structures of bone. Not all of these techniques give the investigator the ability to correlate the mineral content of the bone with its morphology and histometry. For example, light microscopy is the most common imaging tool used to investigate the morphology and histometry of bone. Bulk staining techniques have been reported [34, 35, 38, 55, 76] to enhance the morphologic detail of the tissues. Since these stained specimens are typically ground and polished to 20 to 30 μm in thickness [13], they inherently have overlapping tissue structures and associated projection effect errors. In an attempt to minimize projection effect errors in bone, surface staining techniques [1, 39, 50, 54, 55] have been used. Unfortunately, the lack of inter- and intra-laboratory uniformity of the staining technique can limit morphologic details and accuracy. Furthermore, neither bulk nor surface staining techniques can provide investigators with any quantitative measure of the bone mineral content.

Computed tomography (CT) [29, 32, 47, 51, 64, 66, 71, 75], and microcomputed tomography (microCT) [36, 37, 48, 49], are imaging tools that are being used to help visualize the structure of bone.

MicroCT, a higher resolution imaging technique, can resolve about 40 to 90 μm [33, 36, 48, 49]. However, the size of individual lacunae, canaliculi, and Haversian systems are typically on the order of 7 to 12 μm in size -- roughly 6 times smaller than even microCT can resolve. Finally, as with light microscopy, neither CT nor microCT can provide the investigator with quantitative mineral content information of the bone at the microscopic level.

The mineral content of bone has been measured using various techniques [70]. The mineral content of relatively large bone specimens can be measured by either ashing [8, 25], using chemical assays [8], or by photon absorptiometry [2, 14, 15, 23, 26, 43, 52, 61, 65, 74]. While these techniques can determine the mineral content of bone tissues, none are able to accurately measure the mineral content of an individual osteon or trabecula at the microscopic level.

Microradiography is a technique that has been used for over four decades to quantify the microscopic mineral content changes in cortical bone [31, 44, 45, 46, 50, 55, 56, 73, 77, 78]. The graylevel contrast in microradiography is based primarily on the incident beam attenuation by the mineral content of the specimen. The greater the amount of mineral in the tissue, the fewer the number of X-rays passing through the bone specimen and the whiter the image. Jowsey et al. [45, 46] have recommended that sections of cortical bone be ground and polished to 100 μm in thickness to obtain optimal visualization of the morphologic, histometric, and mineral content of the bone. However, since cancellous bone specimens of this thickness inherently have overlapping trabeculae and projection effect errors, the use of microradiography for correlative morphologic, histometric, and mineral content analysis of cancellous bone has been avoided.

Backscattered electron (BSE) imaging is a relatively recent application of the scanning electron microscope (SEM) that is being advocated by biomaterial, orthopaedic, and bone researchers [3, 4, 5, 6, 10, 11, 12, 16, 17, 18, 19, 20, 21, 22, 42, 58, 59, 67]. Backscattered electrons are high energy electrons that penetrate into the surface of the bone specimen approximately 5 μm [18, 58, 67, 68] and reflect back to the BSE detector. It has been well established that the number of electrons reflected from the surface layer of pure elements or compounds are proportional to its average atomic number [7, 9, 10, 24, 40, 53, 62, 63, 67, 68]. Specimens with a higher average atomic number reflect a greater fraction of backscattered electrons producing whiter BSE image graylevels in biomaterials and bone. Conversely, specimens with a lower average atomic number reflect a smaller fraction of backscattered electrons and display darker BSE image graylevels. Not only is the BSE signal proportional to the average atomic number, but work by Skedros et al. [67, 68] has shown that the BSE signal is proportional to the bone mineral content and density (g/cc).

Recently, three teams of investigators [11, 42, 72] have shown the advantages of using the BSE imaging techniques to describe the morphologic detail and to accurately quantify the histometry of cancellous bone and biomaterials. These investigators [11, 42, 72] have all concluded that the projection effect errors caused by the tissue overlap in bone, are minimized with the BSE imaging techniques. However, they have limited their comparative studies of projection effects only to the morphology and histometry of bone. To date, there has not been a correlated BSE and microradiographic study that investigates how tissue overlap influences the graylevel distribution measured mineral content data of bone.

Using correlated microradiographic and BSE imaging techniques, the objective of this study is to document any errors in the mineral content measurements of bone tissue associated with overlapping bone tissue structures.

## Methods

Cortical and cancellous bone specimens used in this study were supplied by the Division of Radiobiology, University of Utah School of Medicine. The specimens were cross-sections of a vertebral body retrieved from a 3 year old beagle dog. The bone specimens had been dehydrated in ascending grades of alcohols, embedded in polymethyl methacrylate [30], and reduced to an average thickness of 100 μm [45, 46]. Microradiographs of both cortical bone and neighboring cancellous bone were provided on high resolution spectroscopic plates (IMTEC Emulsion Type 1A, Sunneyvale, CA) using a custom made microradiograph unit. The microradiographs with the greatest contrast between the mineral phases of the bone were imaged using a light microscope (Nikon Optiphot, Nikon Inc., Garden City, New York) equipped with a video camera (Dage Series 68, Dage-MTI, Inc., Michigan City, IN). Using the imaging system described elsewhere [10, 16], unfiltered, digital images of microradiographed cortical bone (Figure 1a) and cancellous bone (Figure 2a) were captured and stored for subsequent image analysis [10].

After microradiography, the top surface of each embedded bone specimen was sputter coated with a thin layer of gold at 100 mTorr for 60 seconds (Hummer, Model VIA, Technics Inc., Alexandria, VA). The gold coated bone specimens were placed into the chamber of an SEM (JEOL T-330A, JEOL USA, Inc., Peabody, MA) equipped with a pair of semiconductor BSE detecting elements (T300-BE152 Backscattered Electron Detector, JEOL Technics LTD., Tokyo, Japan) and imaged at 30 kV, 100 μA at a working distance of 15 mm. The brightness and contrast of the SEM were set such that the weighted mean graylevels (WMGLs) of the BSE bone images were calibrated [16] with the WMGLs of the identical regions of the microradiographic images. Unfiltered, digital BSE images of cortical bone (Figure 1b) and cancellous bone (Figure 2b) were captured [10, 16], at the magnification and locations that matched the microradiographic images. The morphology of bone was observed and qualitatively compared between the two imaging techniques.

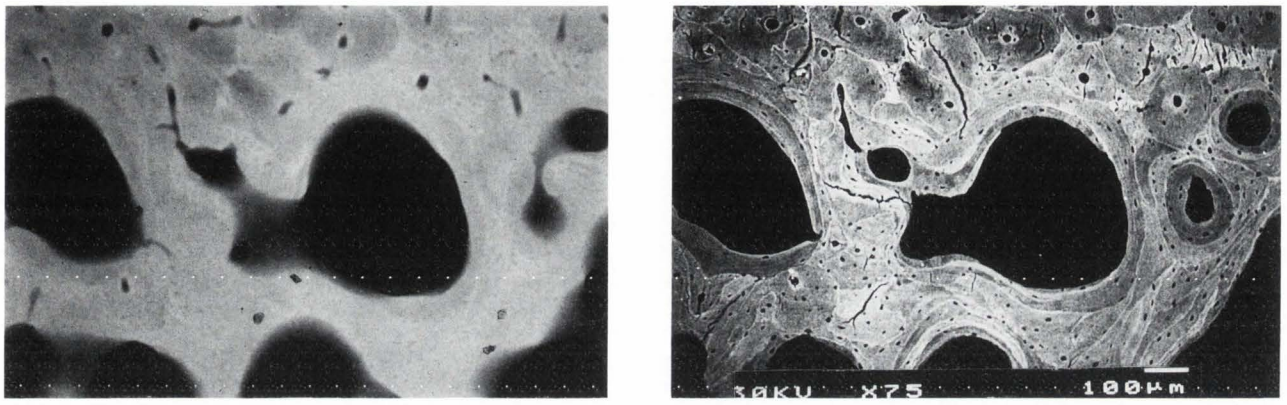


(a) (b)

Figure 1: Comparison of the same region of canine cortical bone imaged using (a) microradiography and (b) backscattered electron imaging techniques. Note the increased image resolution of the backscattered image.

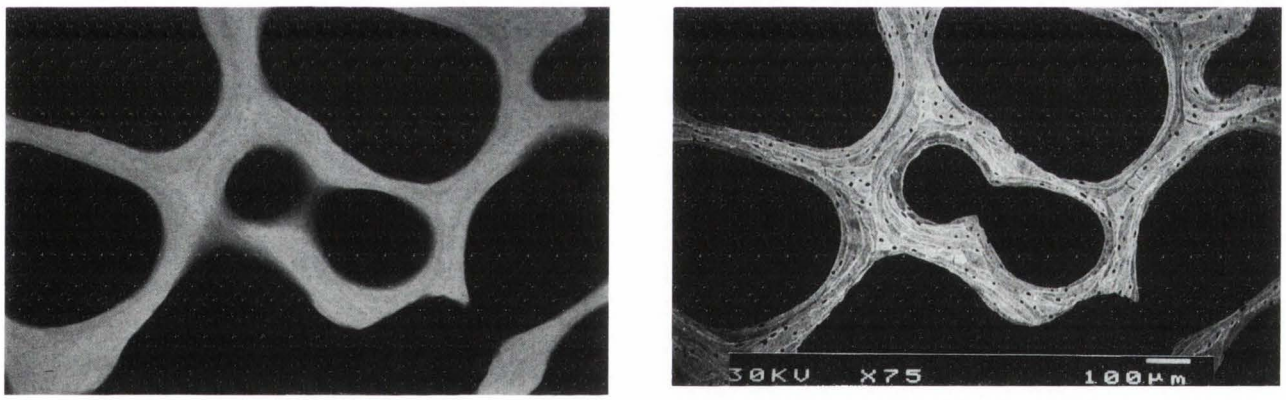


(a) (b)

Figure 2: Comparison of the same region of canine cancellous bone imaged using (a) microradiography and (b) backscattered electron imaging techniques. Note the increased image resolution of the backscattered image.

Each of the 512 by 570 pixels of the captured image [10] had an associated integer value (range 0 to 255) which designated the graylevel intensity. Black pixels on the image have a value of 0, while the brightest white pixels have the value 255. The remaining values between 1 and 254 represented discrete shades of gray from near-black to near-white. Analysis of the images was controlled by using microcomputer-based software routines. Bony regions with distinctive structural features were chosen for comparison of the histometric parameters -- bone surface perimeter and bone area -- between the digital images captured from the microradiographic and BSE techniques. The histometry program used a thresholding technique [28] which allowed the operator to select the appropriate graylevels of the images that represented bone. The area and surface perimeter of the selected regions were measured and recorded.

As with the histometric measurements, the mineral content analysis of the images was controlled by using a microcomputer-based software routine. The mineral content program also used the thresholding technique [28] to select the appropriate graylevels of the images that represented bone. The 256 graylevels of each image were grouped into 51 subranges or "bins" (i.e., graylevels 0-5, 6-10, 11-15, ..., 251-255). In this manner, graylevel sensitivity could be maintained while significantly reducing the analysis time.

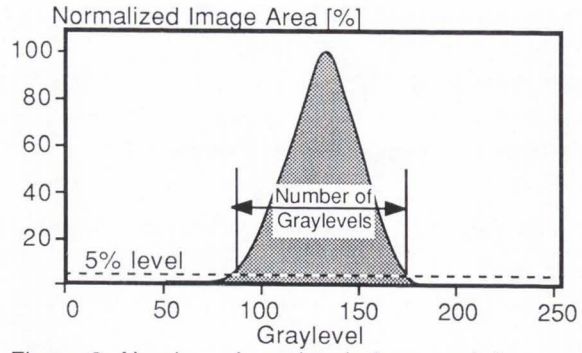


Figure 3: Number of graylevels from each image was determined from measuring the base of the graylevel histogram profile as defined by the 5 percent level.

The result was a series of 51 numbers representing the proportion of the selected region occupied by pixels of each graylevel bin. These numbers may be plotted against graylevel in histogram form to obtain a standard "image graylevel histogram" [28]. A best-fit curve, a graylevel histogram profile (GHP) connecting the values of the histogram, was determined from data collected from seven visually distinct cortical regions and from seven distinct regions of cancellous bone.

The number of graylevels, a measure of the image contrast, was determined from measuring the base of the GHP (Figure 3). The base of a given GHP was defined as the number of graylevels that were a minimum of 5 percent of the peak of the GHP.

Morphological observations were compared qualitatively. The histometric and graylevel data were statistically analyzed using the Mann-Whitney Test for nonparametric, data [27, 69]. Statistical significance was determined with a predefined p-value of less than or equal to 0.05.

## Results

### Morphologic Observations

The BSE imaging technique provided better resolution of both cortical and cancellous bone structures when compared to microradiography (Figures 1, 2). BSE images showed the size and elliptical shape of the lacunae, lamellar patterns and cement lines of the bone. The microradiographic images had less resolution and showed less morphologic details. Using microradiography, the lacunae, lamellae and cement lines of the bone were not as clearly observed as with the BSE technique.

### Histometric Results

The histometric results from this study are presented in Table 1. Measurements from the microradiograph images of cortical bone indicated that the average surface perimeter measured 112.6 ± 1.9 μm (range 109.9 to 115.6 μm) while the average cancellous surface perimeter measured 211.0 ± 55.9 μm (range 126.1 to 312.1 μm). In contrast, measurements from the BSE images of cortical bone showed that the surface perimeter measured 130.8 ± 1.9 μm (range 129.4 to 134.5 μm) while the cancellous region measured 328.2 ± 101.8 μm (range 217.4 to 427.7 μm). The surface perimeters of both the cortical bone (p=0.018) and the cancellous bone (p=0.043) measured using the BSE technique were determined to be significantly greater than the perimeters measured using microradiography.

The microradiographed specimen had 76.1 ± 0.4 square μm (range 75.3 to 76.5 square μm) of cortical area and 39.0 ± 0.3 square μm (range 38.6 to 39.5 square μm) of cancellous bone area. The BSE imaged specimen had 75.9 ± 0.3 square μm (range 75.6 to 76.3 square μm) of cortical area and 30.6 ± 0.2 square μm (range 30.4 to 30.9 square μm) of cancellous bone area. Although BSE did not produce images of cortical bone that were perceivably different (p = 0.237) than microradiography, the BSE images did have significantly less (p=0.018) cancellous bone area than the microradiographed image from the identical regions.

### Mineral Content Results

The GHPs of the calibrated images are presented in Figures 4a and 4b. The WMGLs measured from the images of the bone are listed in Table 2. The microradiographs had an average WMGL of 59 ± 13 (range 35 to 73) for the cortical bone regions and 111 ± 6 (range 102 to 119) for the cancellous bone regions. Matching regions from the BSE images had an average WMGL of 64 ± 15 (range 42 to 87) for the cortical bone regions and 101 ± 13 (range 85 to 119) for the cancellous bone regions. Statistically, there was no measurable differences between the WMGLs of the microradiographs and the BSE images for either the cortical bone (p=0.447) or the cancellous bone (p=0.178). This confirmed that the WMGLs from the BSE images were calibrated with the WMGLs of the microradiographs.

The number of detectable graylevels (Table 2) from the microradiographs averaged 21 ± 6 (range 15 to 30) for the cortical bone and 24 ± 2 (range 20 to 25) for the cancellous bone. The number of detectable graylevels from the BSE images averaged 43 ± 6 (range 35 to 50) for the cortical bone and 37 ± 13 (range 15 to 50) for the cancellous bone. The BSE images had significantly more graylevel contrast than the microradiographs for both the cortical (p=0.018) and cancellous (p=0.046) bone.

## Discussion

The observations of this study showed that the BSE technique could more accurately discriminate the morphology, histometry, and mineral content in bone. The morphologic observations confirmed the reports made by previous investigators [11, 42, 72]. The BSE technique provided substantially better resolution of the bone morphology and had less projection effect errors when compared with microradiography. The surface perimeters of both the BSE imaged cortical and cancellous bone were, as previously reported [11, 42, 72], substantially greater than the surface perimeters measured from the microradiographic images. This greater amount of surface perimeter found in the BSE images of bone was attributed to the noticeably better resolution of the images.

TABLE 1: Bone surface perimeter and bone area of the specimen imaged using microradiography (μRad) compared with the same region imaged using backscattered electron (BSE) imaging. The mean, one standard deviation (STDS), minimum (MIN), maximum (MAX), and p-values are given. Significant differences ($p \leq 0.05$) between the microradiographic and BSE imaging techniques are indicated by an asterisk (*).

| Region Number | Cortical Bone | | | | Cancellous Bone | | | |
|---|---|---|---|---|---|---|---|---|
| | Perimeter (μm) | | Area (sq.μm) | | Perimeter (μm) | | Area (sq.μm) | |
| | μRad | BSE | μRad | BSE | μRad | BSE | μRad | BSE |
| 1 | 113.0 | 129.4 | 75.3 | 75.6 | 126.1 | 383.1 | 39.0 | 30.9 |
| 2 | 111.0 | 131.5 | 76.5 | 76.1 | 199.1 | 409.2 | 38.9 | 30.4 |
| 3 | 114.0 | 129.4 | 76.2 | 75.6 | 201.0 | 427.7 | 39.3 | 30.4 |
| 4 | 115.6 | 134.5 | 75.9 | 76.1 | 199.7 | 225.9 | 39.5 | 30.6 |
| 5 | 112.0 | 130.3 | 76.5 | 75.6 | 199.1 | 217.5 | 39.0 | 30.6 |
| 6 | 112.5 | 131.4 | 75.9 | 76.3 | 239.6 | 217.4 | 38.8 | 30.7 |
| 7 | 109.9 | 129.4 | 76.5 | 76.1 | 312.1 | 416.3 | 38.6 | 30.6 |
| MEAN | 112.6 | 130.8 | 76.1 | 75.9 | 211.0 | 328.2 | 39.0 | 30.6 |
| STDS | 1.9 | 1.9 | 0.4 | 0.3 | 55.9 | 101.8 | 0.3 | 0.2 |
| MIN | 109.9 | 129.4 | 75.3 | 75.6 | 126.1 | 217.4 | 38.6 | 30.4 |
| MAX | 115.6 | 134.5 | 76.5 | 76.3 | 312.1 | 427.7 | 39.5 | 30.9 |
| p-value | *0.018 | | 0.237 | | *0.043 | | *0.018 | |

TABLE 2: Comparison of the number of graylevels of identical regions of bone obtained using microradiography and backscattered electron (BSE) imaging. The mean, one standard deviation (STDS), minimum (MIN), maximum (MAX), and p-values are given. Significant differences ($p \leq 0.05$) between the microradiographic and BSE imaging techniques are indicated by an asterisk (*).

| Region Number | Weighted Mean Graylevel (WMGL) | | | | Number of Graylevels | | | |
|---|---|---|---|---|---|---|---|---|
| | Cortical Bone | | Cancellous Bone | | Cortical Bone | | Cancellous Bone | |
| | μRad | BSE | μRad | BSE | μRad | BSE | μRad | BSE |
| 1 | 72 | 77 | 113 | 114 | 15 | 45 | 25 | 40 |
| 2 | 67 | 58 | 107 | 119 | 20 | 35 | 25 | 40 |
| 3 | 73 | 69 | 102 | 102 | 25 | 45 | 20 | 15 |
| 4 | 52 | 56 | 108 | 85 | 25 | 35 | 25 | 45 |
| 5 | 35 | 42 | 112 | 95 | 20 | 50 | 25 | 25 |
| 6 | 57 | 56 | 115 | 86 | 30 | 45 | 25 | 50 |
| 7 | 56 | 87 | 119 | 107 | 15 | 45 | 20 | 45 |
| MEAN | 59 | 64 | 111 | 101 | 21 | 43 | 24 | 37 |
| STDS | 13 | 15 | 6 | 13 | 6 | 6 | 2 | 13 |
| MIN | 35 | 42 | 102 | 85 | 15 | 35 | 20 | 15 |
| MAX | 73 | 87 | 119 | 119 | 30 | 50 | 25 | 50 |
| p-value | 0.447 | | 0.176 | | *0.018 | | *0.046 | |

Contrary to the literature, the data from this study did not indicate that microradiographs always have larger bone area measurements than the corresponding BSE images [11, 42, 72]. Depending upon the bone's 3-dimensional structure, the amount of overlapping tissue layers, and the X-ray techniques used, microradiography can give the investigator either the same, less, or more bone area when compared to BSE images -- depending upon the individual bone specimen, section, and field selected. If the specimen is a solid piece of cortical bone, microradiography and BSE can give similar bone area results. However, when cortical bone has fairly large voids that occur below the surface of the bone specimen, potential histometric errors can occur. For example, the amount of X-rays that would be needed to properly expose the thick regions of cortical bone could over penetrate thin regions of bone.

Finally, recall that when looking down onto multilayered objects, the resulting boundary is defined by the widest projection of the overlapped structures [41]. If there is less bone on the specimen surface than results from the summation of the individual layers, there will be an impression of more bone present than actually there. This phenomenon was described by Holmes et al. [42], Bloebaum, et al. [11] and Sumner, et al. [72] when they showed that microradiographic images have more bone area than BSE images. All three investigators found regions with less bone on the top surface of the specimen that had been BSE imaged than the summation of the individual layers using the microradiographic technique. This gave the impression that there was more bone present in the microradiographic bone

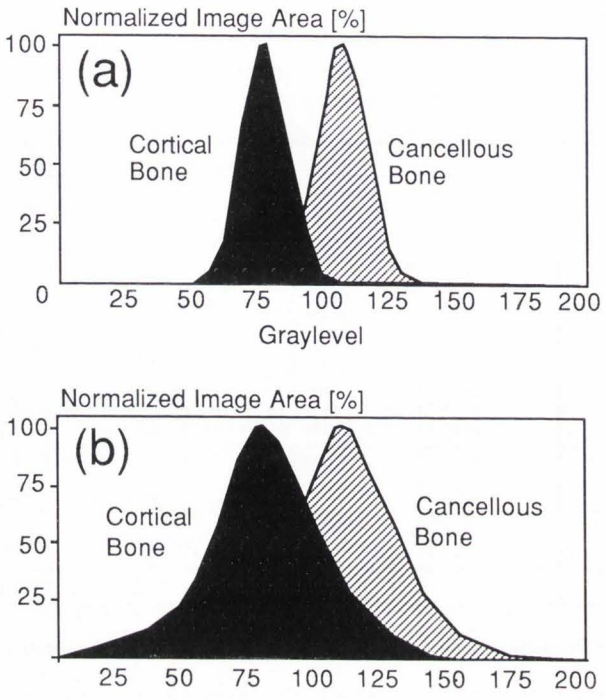


Figure 4: Graylevel histogram profiles of the (a) microradiographic images of cortical and cancellous bone and (b) BSE images of cortical and cancellous bone. Graylevel calibration of the two imaging techniques was accomplished by adjusting the BSE brightness and contrast to give similar weighted mean graylevels the cortical and cancellous bone.

image than in the BSE image. Cancellous bone, being made up of many individual trabeculae, can especially be a problem.

Especially unique to this study was the data showing that projection effect errors can affect the mineral content measurements of bone. Work from our lab [67, 68] has demonstrated that the BSE graylevels of bone are proportional to the mineral content and density (g/cc) of the tissue. The data from this study showed that the BSE images can discriminate significantly more graylevels than the microradiographs. This is because the thickness of the microradiographed specimens tends to mask the multiple mineral phases by averaging the graylevel information over the entire 100 μm thickness of the specimen.

The regions of superimposition of the tissues image using microradiography may appear to have incorrect mineral content values. Just as with the histometric measurements, over and under penetration of the X-ray beam through the 100 μm thick specimen can seriously distort the mineral content measurements, even using calibrated techniques [16, 67, 68]. The same overlapping tissue structures imaged using BSE would appear much differently. Since the electrons only pass through the first few μm [42, 57, 67, 68] of the specimen surface, the structure would not only have more contrast in the graylevel images, but also show the correct mineral content of the individual microscopic structures using published calibration methods [16, 67, 68]. Although using the BSE technique would require a large number of stereologic planes to be analyzed to obtain information from a specimen, correct mineral content data, with good contrast, could be measured throughout the entire specimen without concerns of artifacts caused by projection errors inherent in microradiography.

Correlating the morphologic, histometric, and mineral content of bone at the interface of biomaterials continues to be a goal in biomaterials and basic bone research. Using the BSE mode of the SEM can give investigators the ability to overcome the resolution limitations of the other imaging techniques [1, 8, 25, 31, 35, 36, 37, 46, 47, 48, 49, 51, 54, 55, 56, 64, 66, 70, 73, 75, 76, 77, 78] currently used to measure the bone response to biomaterials.

## Acknowledgment

We wish to thank the Department of Veterans Affairs Medical Center, Salt Lake City, Utah for the financial support of this project. We offer special thanks to S. C. Miller, Ph.D. and the research team at the Division of Radiobiology, University of Utah School of Medicine for supplying the prepared bone specimens and microradiographs used in this study.

## References

1. Allison RT, Sugar AW (1990) Production of high quality ground sections of bone containing metal implants to demonstrate osseo-integration: a simplified method. Med Lab Sci. 47, 168-171.

2. Awbrey BJ, Jacobson PC, Grubb SA, McCartney WH, Vincent LM, Talmage RV (1984) Bone density in women: A modified procedure for measurement of distal radial density. J Orthop Res. 2, 314-321.

3. Bachus K, Bloebaum R, Hofmann A (1990) Minimum trabecular width: the biomechanical limit of load bearing cancellous bone. Trans Orthopaed Res Soc. 15, 54 (abstract).

4. Bachus KN (1992) Superimposition errors when measuring the mineral content of bone. Trans. Orthop. Res. Soc. 17, 111 (abstract).

5. Bachus KN, Baird GO (1992) Correlated compressive strength and stiffness testing with the microstructure of cancellous bone. Trans. Orthopaed. Res. Soc. 17, 558 (abstract).

6. Bachus KN, Hofmann AA, Dauterman LA (1988) Canine and human cancellous bony ingrowth into cobalt chrome and titanium porous coated implants -- a backscattered electron microscopic analysis. Trans Orthopaed Res Soc. 13, 308 (abstract).

7. Ball MD, McCartney DG (1981) The measurement of atomic number and composition in an SEM using backscattered detectors. J Microscopy. 124, 57-68.

8. Biltz RM, Pellegrino ED (1969) The chemical anatomy of bone. J. Bone Joint Surg. 51A, 456-466.

9. Bishop HE (1967) Electron scattering in thick targets. Br J Appl Phys. 18, 703-715.

10. Bloebaum RD, Bachus KN, Boyce TM (1990) Backscattered electron imaging: The role in calcified tissue and implant analysis. J. Biomater. Appl. 5, 56-85.

11. Bloebaum RD, Reid SA, Bachus KN (1989) Backscattered electron imaging in the scanning electron microscope for bone-implant interface analysis. Trans. Orthopaed. Res. Soc. 14, 399 (abstract).

12. Bloebaum RD, Rhodes DM, Rubman MH, Hofmann AA (1991) Bilateral tibial components of different cementless design and materials: Microradiographic, backscattered imaging, and histologic analysis. Clin. Orthop. 268, 179-187.

13. Bloebaum RD, Sanderson C, McCarvill S, Campbell P (1989) Plastic slides in the preparation of implant and tissue for interface analysis. J. Histotechnol. 12, 307-310.

14. Bohr H, Schaadt O (1983) Bone mineral content of femoral bone and the lumbar spine measured in women with fracture of the femoral neck by dual photon absorptiometry. Clin. Orthop. 179, 240-245.

15. Bohr HH, Schaadt O (1987) Mineral content of the upper tibia assessed by dual photon absorptiometry. Acta Orthop. Scand. 58, 557-559.

16. Boyce TM, Bloebaum RD, Bachus KN, Skedros JG (1990) Reproducible method for calibrating the backscattered electron signal for quantitative assessment of mineral content in bone. Scan. Micro. 4, 591-603.

17. Boyde A, Cowham MJ (1980) An alternative method for obtaining converted back-scattered electron images and other uses for specimen biasing in biological SEM. Scanning Electr. Microsc. I, 227-232.

18. Boyde A, Jones S (1983) Backscattered electron imaging of skeletal tissues. Metab. Bone Dis. Rel. Res. 5, 145-150.

19. Boyde A, Maconnachie E, Reid SA, Delling G, Mundy GR (1986) Scanning electron microscopy in bone pathology: Review of methods, potential and applications. Scanning Electr. Microsc. 4, 1537-1554.

20. Boyde A, Reid SA (1983) A new method of scanning electron microscopy for imaging biological tissues. Nature. 302, 522-523.

21. Boyde A, Reid SA (1983) New methods for cathodoluminescence in the scanning electron microscope. Scan Electr Microsc. 4, 1803-1814.

22. Boyde A, Switsur VR, Fearnhead RW (1961) Application of the scanning electron-probe X-ray microanalyzer to dental tissues. J. Ultrastruct. Res. 5, 201-207.

23. Cohn SH, Aloia JF, Letteri JM (1978) Noninvasive measurements of bone mass and their clinical significance. Calcif Tissue Res. 26, 1-3.

24. Cosslett VE, Thomas RN (1965) Multiple scattering of 5-30 keV electrons in evaporated metal films III: Backscattering and absorption. Brit J Appl Phys. 16, 779-796.

25. Currey JD (1984) Effects of differences in mineralization on the mechanical properties of bone. Philos Trans R Soc Lond (Biol). B, 509-518.

26. Dequeker J, Nijs J, Verstraeten A, Geusens P, Gevers G (1987) Genetic determinants of bone mineral content at the spine and radius: A twin study. Bone. 8, 207-209.

27. Devore JL (1982) Probability and Statistics for Engineering and the Sciences, (eds) Brooks/Cole Publishing Company, Monterey, CA, 573-581.

28. Dougherty ER, Giardina CR (1987) Matrix structured image processing. (eds), Prentice-Hall, Englewood Cliffs, NJ, 37-65.

29. Durand EP, Ruegsegger P (1991) Cancellous bone structure: Analysis of high-resolution CT images with the run-length method. J. Comput. Assist. Tomogr. 15, 133-139.

30. Emmanual J, Hornbeck C, Bloebaum RD (1987) A polymethyl methacrylate method for large specimens of mineralized bone with implants. Stain. Technol. 62, 401-410.

31. Engström A (1949) Microradiography. Acta Radiol. 35, 503-521.

32. Faulkner KG, Gluer CC, Majumdar S, Lang P Engelke, K., Genant HK (1991) Noninvasive measurements of bone mass, structure, and strength: current methods and experimental techniques. Am. J. Roentgenol. 157, 1229-1237.

33. Feldkamp LA, Goldstein SA, Parfitt AM, Jesion G, Kleerekoper M (1989) The direct examination of three-dimensional bone architecture *in vitro* by computed tomography. J. Bone Miner. Res. 4, 3-11.

34. Frost HM (1958) Preparation of thin undecalcified bone sections by rapid manual method. Stain Technol. 33, 273-277.

35. Frost HM (1959) Staining of fresh, undecalcified, thin bone sections. Stain Technol. 34, 135-146.

36. Goldstein SA, Feldkamp LA, Ku JL, Champlain FW, Zand M, Jesion G, Ciarelli M, Matthews LS (1986) Architectural effects on trabecular bone material properties. Trans. Orthopaed. Res. Soc. 11, 332 (abstract).

37. Goldstein SA, Ku JL, Kayner DC, Matthews LS (1985) An experimental model for inducing trabecular bone remodeling. Trans. Orthop. Res. Soc. 10, 212 (abstract).

38. Gotfredsen K, Budtz-Jörgensen E, Jensen LN (1989) A method for preparing and staining histological sections containing titanium implants for light microscopy. Stain Technol. 64, 121-127.

39. Gross UM, Strunz V (1977) Surface staining of sawed sections of undecalcified bone containing alloplastic implants. Stain Technol. 52, 217-219.

40. Holliday JE, Sternglass J (1957) Backscattering of 5-20 keV electrons from insulators and metals. J Appl Phys. 28, 1189-1193.

41. Holmes A (1921) Petrographic Methods and Calculations. (eds), D. Van Nostrand Co., New York, 59-63.

42. Holmes RE, Hagler HK, Coletta CA (1987) Thick-section histometry of porous hydroxyapatite implants using backscattered electron imaging. J. Biomed. Mater. Res. 21, 731-739.

43. Jacobson PC, Beaver W, Grubb SA, Taft TN, Talmage RV (1984) Bone density in women: College athletes and older athletic women. J Orthop Res. 2, 328-332.

44. Jowsey J (1955) The use of the milling machine for preparing bone sections for microradiography and microautoradiography. J. Sci. Instruments. 32, 159-163.

45. Jowsey J (1960) Age changes in human bone. Clin. Orthop. 17, 210-218.

46. Jowsey J, Kelly PJ, Riggs BL, Bianco AJ, Scholz DA, Gershon-Cohen J (1965) Quantitative microradiographic studies of normal and osteoporotic bone. J. Bone Joint Surg. [Am]. 47A, 785-806.

47. Kormano M (1989) Imaging methods in examining the anatomy and function of the lumbar spine. Ann. Med. 21, 335-340.

48. Kuhn JL, Goldstein SA, Feldkamp LA, Goulet RW, Jesion G (1990) Evaluation of a microcomputed tomography system to study trabecular bone structure. J. Orthop. Res. 8, 833-842.

49. Layton MW, Goldstein SA, Goulet RW, Feldkamp LA, Kubinski DJ, Bole GG (1988) Examination of subchondral bone architecture in experimental osteoarthritis by microscopic computed axial tomography. Arthritis Rheum. 31, 1400-1405.

50. Lembert E, Galante J, Rostoker W (1972) Fixation of skeletal replacement by fiber metal composites. Clin Orthop. 87, 303-310.

51. Martin RB (1991) Determinants of the mechanical properties of bones. J. Biomech. 24, 79-88.

52. Meade JB (1989) Bone Mechanics, Cowin SC (eds) CRC Press, Boca Raton, FL, 212-251.

53. Niedrig H (1978) Physical background of electron backscattering. Scanning. 1, 17-34.

54. Pilliar RM, Cameron HU, Welsh RP, Binnington AG (1981) Radiographic and morphologic studies of load-bearing porous-surfaced structured implants. Clin. Orthop. 156, 249-257.

55. Plenk HJ (1986) Techniques of Biocompatibility Testing, Williams DF (eds) CRC Press, Boca Raton, Florida, 35-81.

56. Pugh JW, Rose RM, Radin EL (1973) A structural model for the mechanical behavior of trabecular bone. J Biomech. 6, 657-670.

57. Reid SA (1986) Effect of mineral content of human bone on in vitro resorption. Anat. Embryol. (Berl.). 174, 225-234.

58. Reid SA (1986) A study of human skeletal maturation using the scanning electron microscope. Ph.D. Thesis, University College of London.

59. Reid SA, Boyde A (1987) Changes in the mineral density distribution in human bone with age: Image analysis using backscattered electrons in the SEM. J. Bone Miner. Res. 2, 13-22.

60. Richelle LJ, Onkelinx C (1969) Mineral Metabolism: An Advanced Treatise, Comar C, Bronner F (eds) Academic Press, New York, 123-190.

61. Riis B, Thomsen K, Christiansen C (1987) Does calcium supplementation prevent postmenopausal bone loss? J Med New Eng. 316, 173-177.

62. Robinson VNE (1987) Materials characterization using the backscattered electron signal in scanning electron microscopy. Scanning Microsc. 1, 107-117.

63. Robinson VNE, Cutmore NG, Burdon RG (1984) Quantitative composition analysis using the backscattered electron signal in a scanning electron microscope. Scanning Electr. Microsc. 11, 483-492.

64. Ruff CB (1989) New approaches to structural evolution of limb bones in primates. Folia Primatol. (Basel). 53, 142-159.

65. Schaadt O, Bohr H (1982) Non-invasive bone measurements: Methodological problems, Dequeker J, Johnston CC Jr. (eds) IRL Press, Oxford, England, 59-72.

66. Singh S (1989) Ultrasonic non-destructive measurements of cortical bone thickness in human cadaver femur. Ultrasonics. 27, 107-113.

67. Skedros JG, Bloebaum RD, Bachus KN, Boyce TM (1993) The meaning of graylevels in backscattered electron images of bone. J. Biomed. Mater. Res. 27, 47-56.

68. Skedros JG, Bloebaum RD, Bachus KN, Boyce TM, Constantz B (1993) Influence of mineral content and composition on graylevels in backscattered electron images of bone. J. Biomed. Mater. Res. 27, 57-64.

69. Sokal RR, Rohlf FJ (1981) Biometry. The Principles and Practice of Statistics in Biological Research. Wilson J, Cotter S (eds), W. H. Freeman & Co., New York, 114-125.

70. Speller RD, Royle GJ, Horrocks JA (1989) Instrumentation and techniques in bone density measurement. J. Phys. E. Sci. Instrum. 22, 202-214.

71. Stiles RG, Laverina CJ, Resnick D, Convery FR (1990) The calcar femorale. An anatomic, radiologic, and surgical correlative study. Invest. Radiol. 25, 1311-1315.

72. Sumner DR, Bryan JM, Urban RM, Kuszak JR (1990) Measuring the volume fraction of bone ingrowth: A comparison of three techniques. J Orthop Res. 8, 448-452.

73. Takechi H (1977) Trabecular architecture of the knee joint. Acta Orthop. Scand. 48, 673-681.

74. Thompson DD (1980) Age changes in bone mineralization, cortical thickness, and Haversian canal area. Calcif. Tissue Int. 31, 5-11.

75. van Roermund PM, ter Haar Romeny BM, Hoekstra A, Schoonderwoert GJ, Brandt CJ, van der Steen SP, Roelofs JM, Scholten F, Visser WJ, Renooij W (1991) Bone growth and remodeling after distraction epiphysiolysis of the proximal tibia of the rabbit. Effect of electromagnetic stimulation. Clin. Orthop. May, 304-312.

76. Villanueva AR, Lundin KD (1989) A versatile new mineralized bone stain for simultaneous assessment of tetracycline and osteoid seams. Stain Technol. 64, 129-138.

77. Vose GP (1962) Quantitative microradiography of osteoporotic compact bone. Clin. Orthop. 24, 206-212.

78. Williams JL, Lewis JL (1982) Properties and an anisotropic model of cancellous bone from the proximal tibial epiphysis. J Biomech Eng. 104, 50-56.

## Discussion with Reviewers

S.C. Miller: Discussion and comparison of backscatter electron imaging and surface area measurements obtained by light microscopy should specifically indicate that "light microscopy" refers to ground sections and not to routine histological specimens. Histological sections, frequently used for histomorphometry, are often 3 to 7 μm in thickness.
Authors: That is true. However, when analyzing the bone at the interface of many biomaterials, the frailty of the implant specimens limits the minimum thickness to, in many cases, over 10 times the thickness of common histologic specimens.

S. C. Miller: It seems that the primary reason for the difference in gray scale patterns and surface and area measurements in microradiography (particularly in cancellous bone) would be due to section obliqueness.
Authors: The comparisons that were made in this study were between images of the same region of bone using two different techniques. The differences in the histometry and the mineral content are a result of the technique, not the specimens. However, section obliqueness is one the many examples of projection effect errors inherent in thicker specimens.

P. G. T. Howell: How do the graylevels created correlate with mineral content?
Authors: Two recent publications from our laboratory [67, 68] give experimental data for this question. The first study, "The meaning of graylevels in backscattered electron images of bone", uses simulated bone mixtures to model various bone mineral contents. The second study, "Influence of mineral content and composition on graylevels in backscattered electron images of bone" used chicken bone tissue from various embryo, hatchling, 2 week and 1 year of maturity. Together, these two studies show how the graylevels of the BSE images correlate with the bone mineral content.

T. Gruen: There are conventional histomorphometric parameters and it is not clear as to how the histometric parameters in this study compare with the others.
Authors: This study was interested in establishing the potential role of projection effects on the histometry [42] of bone tissue. Measurements of the "bone surface perimeter" and "bone area" were made from a section of embedded bone imaged using microradiography and BSE imaging techniques. We were not attempting to serially section and stereologically reconstruct the entire specimen to obtain the classical histomorphometric parameters of mineralized surface area and mineralized bone volume. It is worth noting that since the histomorphometric and stereologic parameters sum the results over several sections, the projection effect errors measured using microradiography could theoretically accumulate with each section. More research could be conducted to determine the effects of projection effect errors on other histomorphometric parameters. It is the author's opinion that this would likely be unnecessary since there are now several studies [11, 42, 72] showing projection effects with microradiography.

T. Gruen: If the "thick" sections are 100 μm for microradiography, then how can 10 μm lacunae be evident in such thick sections of cortical bone unless they are superimposed on top of each other from top to bottom of the "thick" section?
Authors: Figure 1 of this article illustrates the microradiograph and the BSE images of the cortical bone. Distinct, individual osteocyte lacunae are not clearly observed in the microradiographic image -- only in the BSE image. The "lacunae" that you refer to in Figure 1a are in fact, Haversian canals. These osteonal structures could be imaged using either imaging technique since the canals run throughout the entire 100 μm thick specimen. So depending on the amount of detail needed for the study, the projection effect errors that are associated with microradiography may or may not be an important aspect of the study.

Unidentified Reviewer: Radiographic projection errors are very well known in the literature and are to be expected. The results of the study show that microradiography had more projection errors associated with the morphology and histometry -- a result which can be predicted from pure logic. Projection effects will be increased with decrease in the depth of resolution of any system.
Authors: Before we began this study, we would have agreed with the reviewer's statements. Projection effect errors associated with the morphological and histometric measurements of bone have been investigated and reported in the literature [11, 42, 72]. The objective of this study, as stated at the end of the Introduction, was to "document any errors in the mineral content measurements of bone tissue associated with overlapping bone tissue structures." We feel that the data from this study gave us the ability to achieve this objective. Unexpected to the authors, to the literature, and it seems, to the unidentified reviewer, was "the data from this study did not indicate that microradiographs always have larger bone area measurement than the corresponding BSE images." As the authors indicated in the Discussion, we felt that "Depending upon the bone's 3-dimensional structure, the amount of overlapping tissue layers, and the X-ray techniques used, microradiography can give the investigator either the same, less, or more bone area when compared to BSE images -- depending upon the individual bone specimen, section, and field selected."